Available online at www.sciencedirect.com
ScienceDirect
Journal of Power Sources 173 (2007) 570–577
JOURNAL OF POWER SOURCES
www.elsevier.com/locate/jpowsour

Low-cost synthesis and utilization in mini-tubular electrodes of nano PbO_2

M. Bervas *, M. Perrin, S. Geniès, F. Mattera

Commissariat à l'Energie Atomique, Institut National de l'Energie Solaire, INES-RDI, Parc Technologique de Savoie Technolac, 50 avenue du léman, 73375 Le Bourget du Lac Cedex, France

Received 22 December 2006; received in revised form 1 March 2007; accepted 29 April 2007
Available online 6 May 2007

Abstract

The aim of this work was to explore the possibility of using nano PbO_2 in commercial type tubular lead-acid battery positive electrodes. In that prospect, nanosized αPbO_2 and βPbO_2 have been synthesized at room temperature by a low-cost solution technique involving the chemical oxidation of lead nitrate with ammonium persulfate in concentrated alkaline medium. Mini-tubular electrodes were then prepared using the same type of gauntlet as the one used in commercial tubular electrodes. We show that the capacity and the cycling stability of the tubular electrode highly depend on the sulfuric acid concentration in the electrolyte and on the lead dioxide surface area. A percentage of utilization higher than 45% of the active mass with an excellent cycling stability was obtained when our nano βPbO_2 was used as active material in a diluted H_2SO_4 electrolyte.

Keywords: Nano PbO_2; Lead-acid battery; Low-cost synthesis; Tubular electrode

1. Introduction

With quasi-monopolies on huge markets such as the automobile industry or the storage of renewable energies [1] lead-acid batteries are still today the most sold of the secondary batteries. This is mainly due to their low cost compared to the other technologies. However, many people predict that in the long run the lead-acid battery is bound to disappear and will be completely replaced by rechargeable batteries with higher energy and power densities such as the Ni-MH or the Li-ion. To keep them competitive, it is therefore important to continue the research effort and to investigate new approaches to decrease their manufacturing cost even further.

Several attempts have been made in the past to use chemically prepared PbO_2 in plates [2–4] or tubular [5] positive electrodes. The main advantage of such electrodes over the conventional ones is that the electrochemical formation of the electrodes can be completely suppressed since "precharged" batteries are constructed directly. Although it has often been claimed in the literature that the PbO_2 electrochemical activity is intrinsically lower when it is prepared chemically instead of electrochemically [6], promising results were obtained in those various studies especially when additives, such as graphite, were used [2–5].

It is well known that one way to increase the percentage of utilization of the PbO_2 in the positive electrode is to increase its surface area [7] and it has recently been reported by Morales et al. that percentage of utilization as high as 65% can be obtained with nanosized PbO_2 [8]. This work clearly demonstrated the real interest of using nano PbO_2 as active material in the lead-acid battery positive electrode but its practical usefulness was however limited since the results were obtained on thin film electrodes with a thickness of 70 μm or less, when the thickness of the commercial plates is of a few millimetres [9]. The nano PbO_2 powder was in that case synthesized from the hydrolysis of lead tetraacetate. Several other articles dealing with the chemical synthesis of nanosized or nanostructured PbO_2 have been recently published. They show that it is possible to prepare PbO_2 with tailored morphologies such as: nanorods [10], nanobelts [11], hollow spheres [12] or macroporous nanostructured lead dioxide [13].

In this article, we report on the low-cost synthesis of nanosized α and βPbO_2 and their utilization in mini-tubular electrodes. The nano-lead dioxide was synthesized at room temperature from the chemical oxidation of lead nitrate with

* Corresponding author. Tel.: +33 6 33 47 94 88; fax: +33 4 79 68 80 49.
E-mail address: bervas_mathieu@hotmail.com (M. Bervas).

0378-7753/$ – see front matter © 2007 Elsevier B.V. All rights reserved.
doi:10.1016/j.jpowsour.2007.04.077

ammonium persulfate in alkaline conditions by a solution technique. For the electrochemistry part of this study, the goal was to develop a system that could, when fully optimized, be readily scaled up to be used in real size electrode. Therefore, we prepared small tubular electrodes with gauntlet cut from the gauntlet used in the commercial tubular plates. Our initial results presented here reveal that percentage of utilization of the lead dioxide approaching 45% can be achieved.

2. Experimental

The lead dioxide was prepared from the chemical oxidation of a lead(II) precursor with ammonium persulfate in alkaline conditions. Unless specified otherwise, the lead precursor was lead(II) nitrate. At first, 100 ml of sodium hydroxide at the desired concentration were prepared. Once transparent and cooled, the sodium hydroxide solution was split in half in two beakers, one for the lead precursor and one for the ammonium persulfate, and these two solutions were stirred separately for another hour. The ammonium persulfate solution was then poured slowly into the lead precursor solution and the new solution was stirred either 5 h or overnight, in any case long enough to let the chemical reaction go to completion. Unless mentioned otherwise, the concentration of lead precursor in this final solution was 0.01 M and the concentration of ammonium persulfate 0.012 M. The small excess of ammonium persulfate was introduced to insure the full oxidation of the lead(II) precursor. At the end of the stirring period, the precipitate was filtered, washed with plenty of distilled water, dried in air at 60 °C and finally ground with a pestle in an agate mortar. For the very high NaOH concentration the final filtering was difficult and a slightly different procedure had to be used after the overnight stirring of the lead precursor/$NH_4S_2O_8$ solution in order to increase the yield. The stirring was stopped to let the precipitate sit at the bottom of the beaker, the excess NaOH solution was discarded with a pipette, the precipitate was dried at 60 °C, washed in 250 ml of distilled water, filtered, dried again at 60 °C and ground.

In order to make a comparison with our powders we also synthesized some nano βPbO_2 using the method of Morales et al. [8] which simply consists in vigorously stirring 5 g of lead(IV) acetate in 25 ml of distilled water for half an hour. This type of lead dioxide will be referred to as $nPbO_2$ in this article.

The ammonium persulfate, lead(II) nitrate, lead(II) perchlorate and lead(IV) acetate were all bought from Sigma–Aldrich, the lead(II) acetate came from Prolabo and the lead(II) nitrate was from Merck. All of them were used as received without any further treatment.

Mini-tubular positive electrodes were then prepared with the nanosized PbO_2 as active material. A microporous polyethylene film was placed along the inside wall of the gauntlet to prevent our powder from dispersing into the electrolyte [5]. The gauntlet was filled with 400 mg (unless mentioned otherwise) of PbO_2 powder, without any mechanical pressure, and then with sulfuric acid at $d = 1.03$. The 2.5 cm high gauntlet was closed at the bottom by its cap and at the top by a piece of AGM separator. The cap at the bottom of the gauntlet was firmly held in place by the current collector, a pure lead spine of the same diameter as the inside diameter of the cap. A thermoretractable tube was placed on the current collector just above the gauntlet to minimize the corrosion of the lead by the sulfuric acid during cycling. A picture and a cross-section schematic of the mini-tubular electrode are presented in Fig. 1.

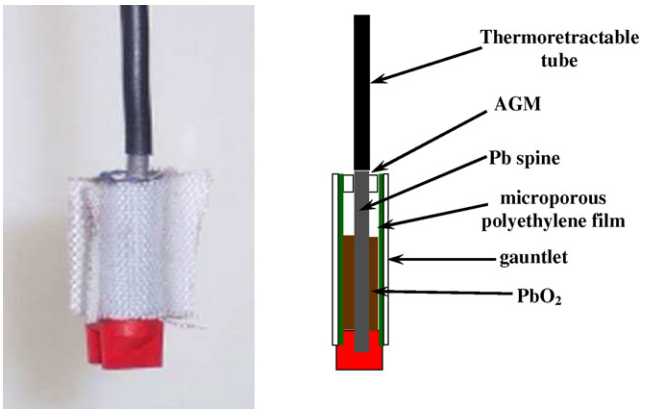

Fig. 1. Picture and cross-section schematic of the mini-tubular electrode used in this study.

The tubular electrode was cycled in a laboratory glass cell against a small conventional negative electrode cut from a commercial plate. The negative electrode active mass was in large excess compared to the positive electrode active mass. All the results presented in this article were obtained in galvanostatic mode at a current of ±0.01 A (i.e. current density of 25 mA g^{-1} of PbO_2). The cut-off voltage at the end of the discharge depended on the density of the sulfuric acid electrolyte: 2 V versus $Pb^0/PbSO_4$ for $d = 1.28$, 1.9 V versus $Pb^0/PbSO_4$ for $d = 1.20$, 1.8 V versus $Pb^0/PbSO_4$ for $d = 1.12$ and 1.6 V versus $Pb^0/PbSO_4$ for $d = 1.03$. In each case, this corresponded to a voltage of about 100 mV below the discharge plateau.

The percentage of utilization of the PbO_2 was evaluated with respect to a 100% theoretical capacity of 224 mAh g^{-1}.

3. Synthesis of the lead dioxide

Morales et al. have shown recently that nanosized βPbO_2 can be synthesized readily at room temperature from lead tetraacetate and water [8]. However, we wanted to find another route to prepare our nano PbO_2 powder since lead tetraacetate is an expensive precursor. We were also interested in synthesizing nanosized αPbO_2 in addition to βPbO_2 since it has been reported that higher percentage of utilization of the PbO_2 in the positive electrode of the lead-acid battery are obtained when the α phase is used instead of the β phase [7]. As will be reported in this section, both of these goals were achieved when the lead dioxide was synthesized by the chemical oxidation of lead(II) precursors with ammonium persulfate in sodium hydroxide [14]. The details of the synthesis procedure are provided in Section 2. A comparison of the prices of the lead tetraacetate and of the precursors we investigated is provided in Table 1. It is clear that the overall cost reduction for the synthesis of the nano PbO_2 is very

Table 1
Prices of the different compounds used in this study (taken from Sigma–Aldrich)

Compound	Purity (%)	Quantity (g)	Price (€)
$Pb(CH_3COO)_4$	>99.99	25	234
$Pb(NO_3)_2$	>99	500	36
$Pb(C10_4)_2{\cdot}3H_2O$	98	500	170
$Pb(CH_3COO)_2{\cdot}3H_2O$	>99	500	36
$(NH_4)_2S_2O_8$	>98	500	26
NaOH	>97	500	13

significant even when the prices of ammonium persulfate and the sodium hydroxide are taken into account.

Three types of divalent lead precursors were tested: lead nitrate $Pb(NO_3)_2$, lead perchlorate trihydrate $Pb(ClO_4)_2{\cdot}3H_2O$ and lead acetate trihydrate $Pb(CH_3COO)_2{\cdot}3H_2O$. For those three batches the concentration of the lead(II) precursor was 0.005 M, the concentration of the ammonium persulfate 0.01 M and the concentration of the sodium hydroxide 1 M. The sodium hydroxide solution containing both the precursor and the oxidant was stirred for 5 h, stirring period at the end of which a black precipitate is formed. In all three cases the black powder obtained after filtration and washing of the precipitate was pure αPbO_2. This has been confirmed by X-ray diffraction (XRD), as shown in Fig. 2.

Two chemical reactions are involved in the formation of the lead dioxide [10]. The first one is brought about by the sodium hydroxide and results in the transformation of the lead(II) precursor into a lead hydroxide compound:

$$PbX_2 + 3OH^- \rightarrow Pb(OH)_3^- + 2X^- \quad (1)$$

with $X = (NO_3)^-$, $(CH_3COO)^-$ or $(ClO_4)^-$

The second reaction is the oxidoreduction reaction between the lead hydroxide and the persulfate anions according to:

$$Pb(OH)_3^- + OH^- \longrightarrow PbO_2 + 2e^- + 2H_2O \quad (2a)$$

$$S_2O_8^{2-} + 2e^- \longrightarrow 2SO_4^{2-} \quad (2b)$$

$$Pb(OH)_3^- + S_2O_8^{2-} + OH^- \rightleftharpoons PbO_2 + 2SO_4^{2-} + 2H_2O \quad (2c)$$

The narrow widths of the XRD peaks on the three patterns presented in Fig. 2 indicate that the crystallites size of the αPbO_2 obtained are of macro-dimensions. The BET surface areas of two of the three PbO_2 samples were measured and the results are presented in Table 2. As expected for macrosized powders,

Table 2
BET surface area our different PbO_2 samples

Compound (lead precursor, NaOH concentration)	Surface area ($m^2\ g^{-1}$)
αPbO_2 (perchlorate, 1 M)	0.95
αPbO_2 (nitrate, 1 M)	1.72
αPbO_2 (nitrate, 6 M)	0.64
βPbO_2 (nitrate, 8 M)	26.43
Positive active material from a commercial plate	4.31
βPbO_2 from $Pb(CH_3COO)_4$	32.8

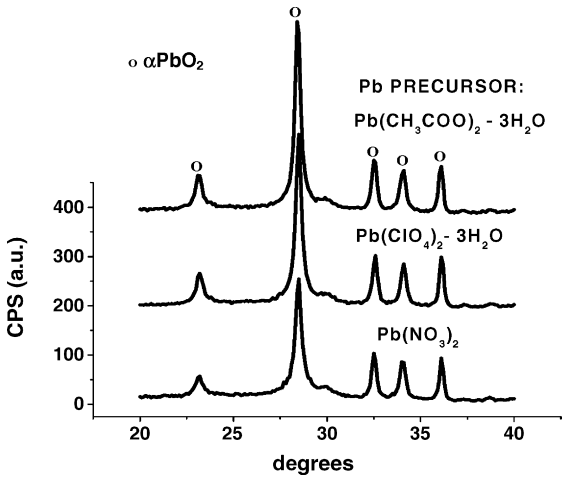

Fig. 2. XRD patterns of the macro αPbO_2 powders obtained from the chemical oxidation of three different lead(II) precursors with ammonium persulfate in [NaOH] = 1 M.

the surface area values obtained were rather low: respectively 1.72 $m^2\ g^{-1}$ and 0.95 $m^2\ g^{-1}$ for the nitrate and the perchlorate precursors.

The sodium hydroxide concentration in the solution was varied in order to change the nucleation and growth kinetics of the PbO_2 particles. Since αPbO_2 can be synthesized successfully from the three precursors tested previously, we focused on the cheapest of the three, namely the lead nitrate. For all of this study on the influence of the NaOH concentration on the PbO_2 crystallites size, only the NaOH concentration of the alkaline solution was changed and all the other parameters were kept constant. Hence the $[Pb(NO_3)_2]/[(NH_4)_2S_2O_8]$ ratio was fixed at 5/6 with a lead nitrate concentration of 0.010 M and a ammonium persulfate concentration equal to 0.012 M. In all cases the solution containing both the lead nitrate and the oxidant was stirred overnight.

Fig. 3 presents the XRD patterns of the powders obtained with sodium hydroxide concentrations lower than 1 M. A different compound, which has been identified as $PbSO_4$ by XRD, is formed at these low NaOH concentrations. The $[PbSO_4]/[\alpha PbO_2]$ ratio increases when the sodium hydroxide concentration decreases and at a sodium hydroxide concentration of 0.05 M, the $PbSO_4$ is almost pure. This result suggests that when the sodium hydroxide concentration is too low, reaction (1) does not take place. Since the lead hydroxide intermediate is not formed, reaction (2c) cannot occur either and there is no oxidoreduction reaction involving the lead cations, which remain in their 2+ valence state.

The XRD patterns of the lead dioxide powders obtained with sodium hydroxide concentrations greater than 1 M are shown in Fig. 4. The αPbO_2 XRD peaks clearly broaden when the NaOH concentration is increased, indicating that the crystallites size decreases. There is however no linear relation between the concentration and the crystallites size since the breadth of the peak is approximately the same for all concentrations between 2 M and 7 M. Surprisingly, a few peaks characteristic of $Pb(NO_3)_2$ can be seen on the XRD patterns of the samples synthesized at NaOH concentrations 2 M and 3 M, and on these two patterns

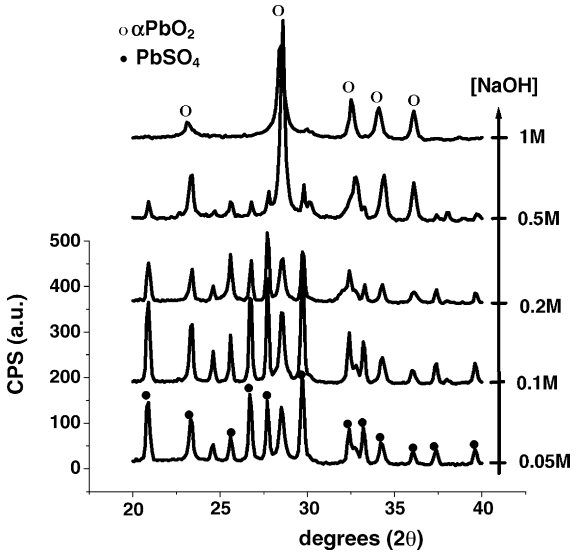

Fig. 3. XRD patterns of the precipitate obtained from the chemical oxidation of lead(II) nitrate with ammonium persulfate in [NaOH] < 1 M. At these low sodium hydroxide concentrations lead sulfate in formed.

only. We do not know at that point why part of the lead precursor remains unreacted at those two concentrations.

As can be seen in Fig. 4, when the sodium hydroxide concentration is higher than 7 M, the lead dioxide formed is not αPbO_2 anymore but βPbO_2. The powder obtained is brown, contrasting with the black colour of the αPbO_2 powder. In the literature, it is usually accepted that the α allotropic phase of the lead dioxide is formed in alkaline conditions, while the β allotropic phase is

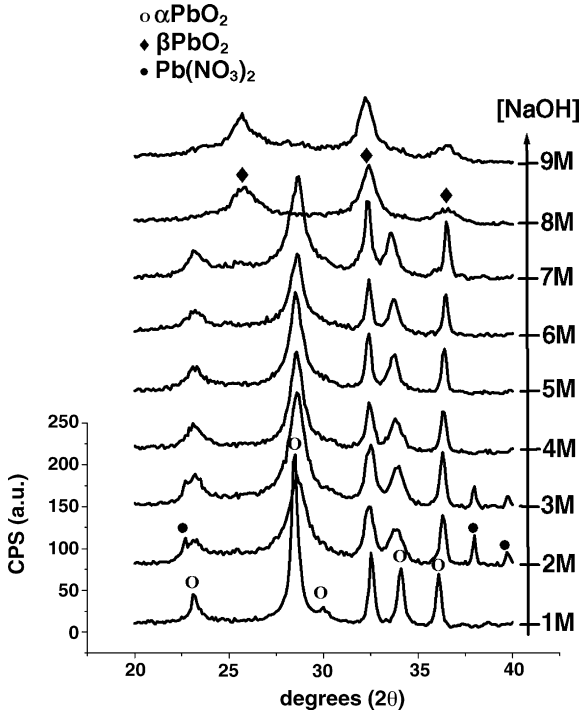

Fig. 4. XRD patterns of the lead dioxide powders obtained from the chemical oxidation of lead(II) nitrate with ammonium persulfate in [NaOH] > 1 M. Nano αPbO_2 is formed for NaOH concentrations between 2 M and 7 M, whereas nano βPbO_2 is obtained for [NaOH] > 7 M.

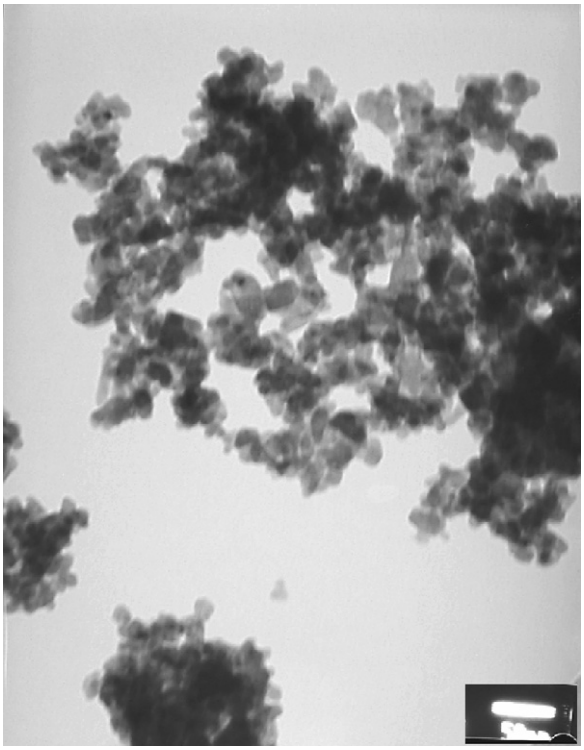

Fig. 5. TEM picture of the αPbO_2 obtained from the chemical oxidation of lead(II) nitrate with ammonium persulfate in [NaOH] = 6 M. The scale bar is 50 nm. The particle size of the αPbO_2 is in the order of 20 nm. This picture also shows the much agglomerated state of the particles, which explains the low surface area of this powder.

formed in acidic conditions [15,16]. The results presented here show that the β phase can also be obtained in strong alkaline conditions.

In Fig. 4, the peaks on the XRD patterns of PbO_2 obtained with NaOH concentration greater than or equal to 2 M are very broad, as one would expect from nano-powders. BET surface area measurements were conducted on two of those batches, αPbO_2 (NaOH 6 M) and βPbO_2 (NaOH 8 M). The results are presented in Table 2. The very high surface area of the βPbO_2 sample (26.4 $m^2\ g^{-1}$) clearly indicates that this is indeed a nano PbO_2. On the contrary the surface area of the αPbO_2 is surprisingly low (0.64 $m^2\ g^{-1}$). Nonetheless the transmission electron microscope (TEM) picture of the αPbO_2 presented in Fig. 5 reveals that the particle size is in the order of 20 nm, thus clearly in the nano-range. The very low surface area of this material is therefore caused by its much-agglomerated state. The agglomerates can be observed on the TEM picture presented in Fig. 5.

These two lead dioxide powders, αPbO_2 (NaOH 6 M) and βPbO_2 (NaOH 8 M), were selected for the preparation of our tubular electrode and will be referred to as $aPbO_2$ and $bPbO_2$ thereafter.

4. Preparation and activation of the tubular electrode

After the filling up of the gauntlet with the lead dioxide and the diluted sulfuric acid, and before the actual utilization of our mini-tubular electrode as a positive electrode in an electrochem-

ical cell, several initial steps had to be performed in order to activate the electrode. After each of those steps, which will be described in this section, the electrode was briefly washed with distilled water.

The first of those initial steps was the creation of a small corrosion layer at the interface between the current collector and the PbO_2 particles. This was carried out by a 20 min long potentiostatic oxidation of the electrode at 2 V versus a platinum grid counter electrode in a sulfuric acid ($d = 1.03$) electrolyte. Similar to what happens in conventional lead-acid battery positive electrode [17,18], it was found that the corrosion layer at the interface between the current collector and the active material is a key component of the electrode and is absolutely necessary to establish the electrical contact between its constituents. The small oxygen outgassing occurring during this potentiostatic step may also have a positive impact on the structure of the active mass by increasing its porosity due to the evacuation of the small bubbles through the PbO_2 particles network.

In most cases, a cell was then assembled with the tubular electrode and a small conventional negative electrode and left for 15 h at open circuit voltage. As shown in Fig. 6, during the rest period the cell voltage increases progressively from its initial value of about 1.7 V and eventually reaches a plateau. As expected, the voltage of this plateau depends on the electrolyte density: approximately 2.12 V versus $Pb^0/PbSO_4$ with H_2SO_4 at $d = 1.28$, 2.05 V versus $Pb^0/PbSO_4$ with H_2SO_4 at $d = 1.20$, 1.98 V versus $Pb^0/PbSO_4$ with H_2SO_4 at $d = 1.12$ and 1.88 V versus $Pb^0/PbSO_4$ with H_2SO_4 at $d = 1.03$. Although the presence of this plateau and its voltage value were very reproducible, the way this plateau was reached varied quite significantly from one sample to the other. Thus, in some cases the voltage of cell increases sharply during the first couple of hours before it enters the plateau (see curves a and d in Fig. 6) and in some others it increases very slowly and with different slopes, slopes that may even be negative by moments (curves b and d in Fig. 6). These noticeable differences from one electrode to the other were observed even when the same electrolyte was used (curves a and b in Fig. 6). The voltage increase is clearly caused by the progressive diffusion of the acid from the electrolyte to the core of the gauntlet. When the concentration gradient between the acid in the active mass porosity and the one in the electrolyte has been balanced, the diffusion stops and the system enters a steady state which causes the voltage plateau on the $E(t)$ curve. The time needed to reach this steady state varies from one sample to the other, reflecting the differences in their porosity and PbO_2 particles percolation paths. Those differences in the active material macrostructure are not surprising since we did not apply any mechanical pressure when the PbO_2 was introduced in the gauntlet; its degree of compression cannot therefore be exactly the same each time. The discrepancies observed from one sample to the other during the 15 h rest period could not be linked to any noticeable difference in the electrochemical performances of the final electrodes. We decided to implement this 15 h rest period step during the preparation of our tubular electrode to monitor the output voltage of the cell and also in an effort to enhance the reproducibility of our experiments. It turned out that this step was not essential and that, unlike the first step (formation of the corrosion layer) or the last one (curing of the electrode), it could be skipped without affecting the final performances.

The final step in the preparation of our mini-tubular electrode was to leave it for one entire day in an oven at 60 °C, in air. This drying step was essential for the activation of the electrode and this is demonstrated in Fig. 7. This figure represents the percentage of utilization of the active material ($bPbO_2$) during the first 20 cycles. To clearly illustrate the impact of the 1-day drying period on the performances of the electrode the drying in this particular case was not carried out before the first cycle but after the tenth one. Hence before the drying at 60 °C the percentage of utilization of the PbO_2 approaches zero but it immediately reaches a value between 15% and 20% afterward, value which is usual in this electrolyte (H_2SO_4 $d = 1.28$) as will be discussed later. Obviously, this drying step can be compared to the curing process undergone by the traditional lead-acid battery plates during their manufacturing. The process that occurs in our electrode during this drying step is most likely of the same nature as

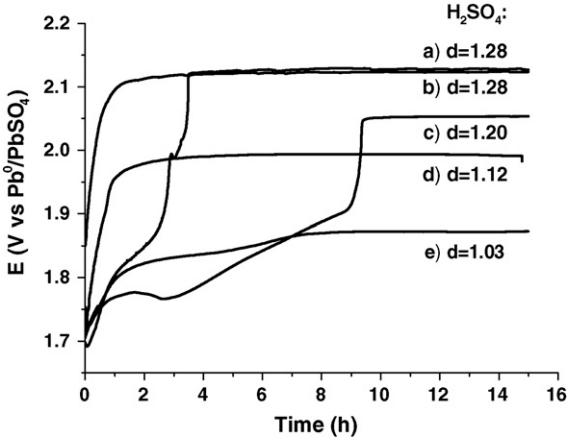

Fig. 6. Evolution of the output voltage in different H_2SO_4 electrolytes of the cells constituted by the mini-tubular electrode at the anode and a piece of conventional negative plate at the cathode during the 15 h rest period implemented during the preparation of the mini-tubular electrodes.

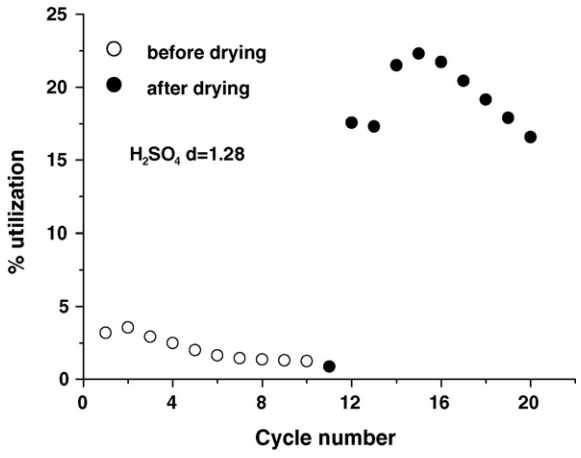

Fig. 7. Percentage of utilization of the $bPbO_2$ in the tubular electrode as a function of the cycle number in H_2SO_4 $d = 1.28$ before and after the 1-day drying at 60 °C.

the one that occurs during the curing of the commercial plates, which is the improvement of the current collector/active mass contact via the oxidation of the metallic lead [18,19].

After this last preparation step, a cell constituted of our tubular electrode at the anode and a small conventional negative plate at the cathode was assembled. It was left for 5 h at open circuit, and the cycling was started.

5. Cycling of the tubular electrode

Fig. 8 presents the evolution of the percentage of utilization of PbO_2 during the first 15 cycles of four mini-tubular electrodes prepared with different types of lead dioxide: $aPbO_2$, $bPbO_2$, $nPbO_2$ and positive active material (PAM) extracted from a commercial plate and hand grounded. The $aPbO_2$, $bPbO_2$, $nPbO_2$ samples were synthesized according to the methods described previously. These electrodes were all cycled in H_2SO_4 at a density of $d = 1.03$. In each case the cycling was started with a discharge and the charge was performed galvanostatically for 3 h at a current of 10 mA. In good agreement with the results of other groups [7,8], this figure indicates that the specific capacity of the lead dioxide is highly dependent on its surface area (cf. Table 2 for the surface area values). Hence the $aPbO_2$ sample, which is composed of nano-particles but has a very low surface area because those particles are agglomerated, does not even reach the 5% of utilization. On the contrary, the two powders with high surface areas have percentage of utilization close to 20%. Two other interesting observations can be made from this graph. The first one is that, in spite of its slightly lower surface area, the $bPbO_2$ synthesized with the cheap lead(II) nitrate precursor exhibits almost the same percentage of utilization as the $nPbO_2$ prepared from the costly lead tetraacetate precursor. The second one is that, when they are used under similar conditions, the specific capacity of a chemically prepared nano PbO_2 significantly exceeds the specific capacity of the PAM used in conventional plates, which confirms the results of Morales et al. [8].

The percentage of utilization exhibited by the PAM in our mini-tubular electrode is very low compared to its usual value

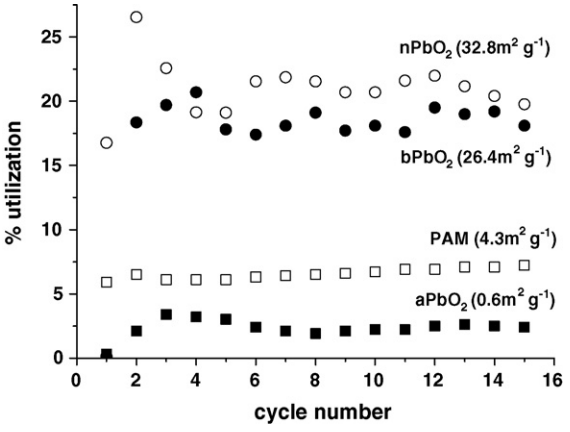

Fig. 8. Percentage of utilization of the PbO_2 in the tubular electrode as a function of the cycle number in H_2SO_4 $d = 1.03$ for four different types of lead dioxide with different surface area.

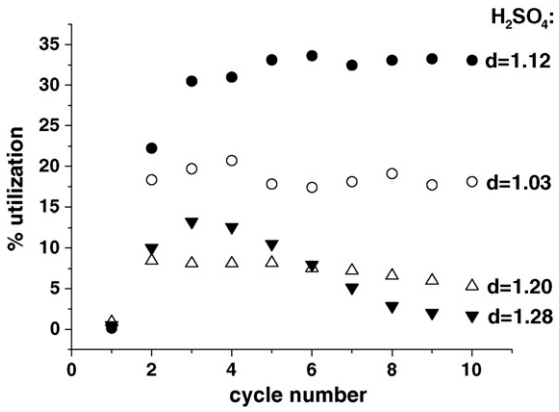

Fig. 9. Percentage of utilization of the $bPbO_2$ in the tubular electrode as a function of the cycle number in four H_2SO_4 electrolytes at different densities.

in conventional plates. This is a due to the destruction of its macrostructure when the PAM was ground prior to its introduction in the gauntlet. In its non-ground state the percentage of utilization of PAM varies between 50% and 58% (at a 20 h discharge rate).

The capacity and the cycling stability of the lead dioxide in our mini-tubular electrode change drastically with the density of the sulfuric acid in the electrolyte. This is illustrated in Fig. 9 that shows the percentage of utilization of the $bPbO_2$ for the first 10 cycles in four electrolytes having different densities: $d = 1.03$, 1.12, 1.20 and 1.28. For each of these four electrodes the cycling was started with a discharge and the charge lasted 3 h at a current of 10 mA. In the two concentrated sulfuric acid electrolytes, not only the electrochemical utilization of the $bPbO_2$ always remains relatively low, but the cycling stability is also very poor since at the end of the 10 cycles the percentage of utilization has already fallen below 5%. On the contrary the cycling stability in the more diluted sulfuric acid is excellent. The percentage of utilization of the PbO_2 is also rather good: about 20% for $d = 1.03$ and between 30% and 35% for $d = 1.12$. Since the positive electrode is small and contains only a limited amount of active material, the most plausible explanation of this experimental observation is that when the sulfuric acid in the electrolyte is too concentrated the ratio $[HSO_4^-]/[PbO_2]$ is too high and causes undesired phenomena, such as for instance some type of sulfate passivation layer, which are highly detrimental to the electrode performances. The situation would be opposite at $d = 1.03$: this ratio would be too low and the number of HSO_4^- available for the discharge reaction would be insufficient to reach high percentage of utilization of the $bPbO_2$. An acid density of 1.12 appears to be a good compromise to maximize the capacity without affecting the cycling stability of the electrode.

As can also be seen in Fig. 9 the first discharge capacity is very small for all the electrodes, independently of the electrolyte, and at least a couple of training cycles is needed.

Figs. 10 and 11 present the percentage of utilization of $bPbO_2$ during discharge in two mini-tubular electrodes submitted to extended cycling. The first one was cycled in H_2SO_4 at $d = 1.12$ and the second one in H_2SO_4 at $d = 1.03$. The electrode used

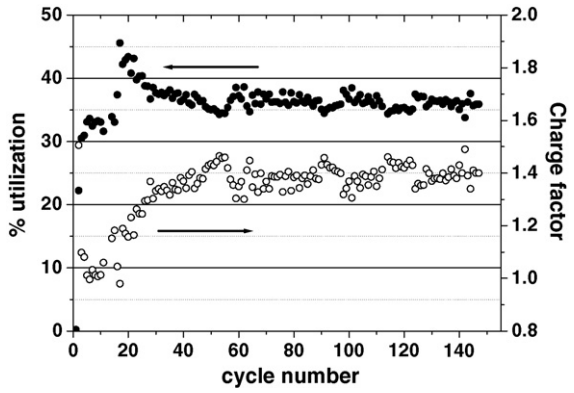

Fig. 10. Percentage of utilization of the $bPbO_2$ in the tubular electrode and charge factor as a function of the cycle number in H_2SO_4 $d = 1.12$. The charge factor is defined as (discharge capacity/previous charge capacity).

for Fig. 11 contained 600 mg of $bPbO_2$ instead of the usual 400 mg so the current density was slightly lower in that case (16.67 mA g^{-1} instead of the usual 25 mA g^{-1}). In both of them distilled water had to be added from time to time in the electrolyte to bring it back to its initial level. Since the charging time had to be adjusted several times during the cycle life we also show on the same graphs the evolution of the charge factor which is defined here as the ratio between the discharge capacity and the previous charge capacity. The important variations of the charge factor at the beginning of the cycle life in Fig. 11 (especially between the cycle numbers 20 and 30) are experimental artifacts caused by an inappropriate programming and have no real physical significance.

These two electrodes exhibit an excellent cycling stability. In H_2SO_4 at $d = 1.12$ the percentage of utilization of the nano PbO_2 quickly stabilizes between 35% and 40% and stays at that level for the next 100 cycles or so. In the electrode cycled in H_2SO_4 at $d = 1.03$ the percentage of utilization increases progressively from its initial value of about 15% to reach somewhere between 45% and 50% where it stabilizes after about 150 cycles. In both cases, there was still no sign of capacity decay when this article was written.

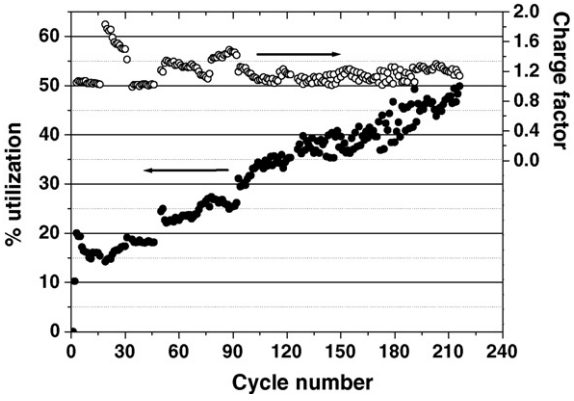

Fig. 11. Percentage of utilization of the $bPbO_2$ in the tubular electrode and charge factor as a function of the cycle number in H_2SO_4 $d = 1.03$. The charge factor is defined as (discharge capacity/previous charge capacity).

We saw previously that an acid density of 1.03 was too low and that due to the lack of HSO_4^- anions in the vicinity of the electrode, much less of the lead dioxide could participate in the discharge reaction during the first cycles than in H_2SO_4 $d = 1.12$. From Fig. 11 we can see that actually during cycling more and more of the $bPbO_2$ gets progressively involved in the discharge reaction and that the capacity eventually reaches a value higher than in H_2SO_4 $d = 1.12$. Higher percentage of utilization of the PbO_2 would then be accessible when the active material becomes progressively active than when it is active early in the cycle life. These two different behaviours observed in Figs. 10 and 11 may also have something to do with the charge factor that was set on average at a lower value in the electrode cycled in H_2SO_4 at $d = 1.03$ (about 1.2) than in the one cycled in H_2SO_4 at $d = 1.12$ (about 1.4) or with the slightly lower current density in the former (16.67 mA g^{-1}) than in the latter (25 mA g^{-1}). More experiments would be needed to clarify these points.

More importantly, these two figures show that excellent cycling stability and percentage of utilization close to the 50% usually obtained in the conventional electrochemically prepared electrodes can be achieved with tubular electrodes filled with chemically prepared nano PbO_2.

The charge and discharge voltage profiles, typical of the $PbO_2 \leftrightarrow PbSO_4$ reaction, for the 210th cycle of the electrode cycled in H_2SO_4 $d = 1.03$ are presented in Fig. 12. The discharge plateau is particularly flat, which is very interesting for practical applications.

According to Pavlov et al. it is the presence of hydrated gel zones within the PbO_2 particles of the conventional lead-acid battery positive plates that make them electrochemically active [20,21]. Moreover, still according to those authors, these gel zones would exchange ions with the electrolyte, thus making the PbO_2 particle an open system and accelerating the reduction of PbO_2 during discharge [22]. Since we have prepared our nano PbO_2 using concentrated NaOH, it is possible that we have obtained by a chemical method PbO_2 particles with a gel–crystal structure, similar to the one obtained by electrochemical formation of PAM, and that it is this structure that is responsible for the electrochemical activity of the chemically obtained PbO_2.

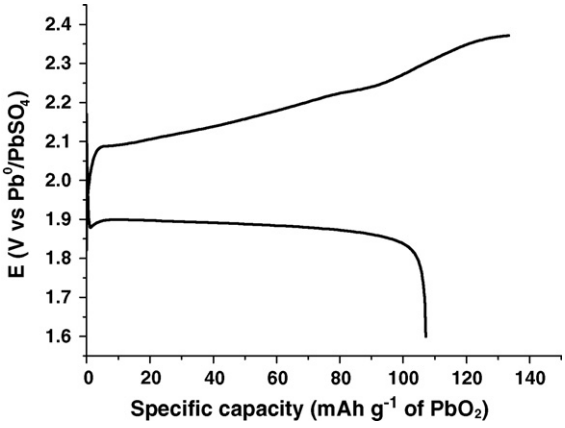

Fig. 12. Charge and discharge voltage profiles of the $bPbO_2$ during the 210th cycle of the electrode used for Fig. 11.

6. Conclusion

We have synthesized nano α and βPbO_2 at room temperature from the chemical oxidation of lead(II) nitrate with ammonium persulfate in strong alkaline conditions. The nano βPbO_2 that is formed in very alkaline conditions exhibits a very high surface area of 26.4 $m^2\ g^{-1}$, making it a particularly attractive lead-acid battery positive electrode active material. This is not the case of the nano αPbO_2 that has a very low surface area due to its much agglomerated state.

More importantly, this synthesis work shows that it is possible to prepare nano PbO_2 from lead nitrate, which is a much cheaper lead precursor than lead tetraacetate. To the best of our knowledge, this is also the first time that it is demonstrated that βPbO_2 can be formed in alkaline conditions.

Mini-tubular electrodes have been constructed using small gauntlets of the type used in commercial tubular electrode. It was found that the electrochemical performances of the mini-tubular electrodes were highly dependent on the surface area of the lead dioxide used as active material and on the sulfuric acid concentration in the electrolyte. In this tubular electrode configuration the nano PbO_2 clearly outperforms the positive active material extracted from a commercial positive plate and percentage of utilization of the positive active material higher than 45% with excellent cycling stability has been achieved with our nano βPbO_2 in diluted H_2SO_4.

Since these mini-tubular electrodes could quite easily be scaled up to real size electrode, these results indicate that it should be possible to assemble precharged lead-acid battery positive electrodes with good performances using nano PbO_2 as active material. Nevertheless it was found that some activation of the electrodes is needed and that the curing and formation of the corrosion layer cannot be completely suppressed.

References

[1] M. Perrin, Y.M. Saint-Drenan, F. Mattera, P. Malbranche, J. Power Sources 144 (2005) 402.
[2] P.T. Moseley, N.J. Bridger, J. Electrochem. Soc. 131 (1984) 608.
[3] E.J. Taylor, G.A. Shia, D.T. Peters, J. Electrochem. Soc. 131 (1984) 484.
[4] E.J. Taylor, G.A. Shia, D.T. Peters, J. Electrochem. Soc. 131 (1984) 487.
[5] S.V. Baker, P.T. Moseley, A.D. Turner, J. Power Sources 27 (1989) 127.
[6] J. Perkins, Mater. Sci. Eng. 28 (1977) 167.
[7] P. Rüetschi, J. Electrochem. Soc. 139 (1992) 1347.
[8] J. Morales, G. Petkova, M. Cruz, A. Caballero, Electrochem. Solid State Lett. 7 (2004) A75.
[9] A. Caballero, M. Cruz, L. Hernàn, J. Morales, L. Sànchez, J. Power Sources 113 (2003) 376.
[10] M. Cao, C. Hu, G. Peng, Y. Qi, E. Wang, J. Am. Chem. Soc. 125 (2003) 4982.
[11] Z.W. Pan, Z.R. Dai, Z.L. Wang, Science 291 (2001) 1947.
[12] G. Xi, Y. Peng, L. Xu, M. Zhang, W. Yu, Y. Qian, Inorg. Chem. Commun. 7 (2004) 607.
[13] P.N. Bartlett, T. Dunford, M.A. Ghanem, J. Mater. Chem. 12 (2002) 3130.
[14] J.P. Carr, N.A. Hampson, Chem. Rev. 72 (1972) 679.
[15] R. Fitas, L. Zerroual, N. Chelali, B. Djellouli, J. Power Sources 58 (1996) 225.
[16] D. Pavlov, in: B.D. McNicol, D.A.J. Rand (Eds.), Power Sources for Electric Vehicles, Elsevier, 1984, p. 163.
[17] B. Monahov, D. Pavlov, A. Kirchev, S. Vasilev, J. Power Sources 113 (2003) 281.
[18] D. Pavlov, in: D.A.J. Rand, P.T. Moseley, J. Garche, C.D. Parker (Eds.), Valve-regulated Lead-Acid Batteries, Elsevier, 2004, p. 83.
[19] A. Ferreira, J. Jordan, J. Wertz, G. Zguris, J. Power Sources 133 (2004) 39.
[20] D. Pavlov, I. Balkanov, T. Halachev, P. Rachev, J. Electrochem. Soc. 136 (1989) 3189.
[21] D. Pavlov, J. Electrochem. Soc. 139 (1992) 3075.
[22] D. Pavlov, I. Balkanov, J. Electrochem. Soc. 139 (1992) 1830.